The Transmembrane State of Antimicrobial Piscidin in Bacterial Cell Membrane Mimics Dramatically Alters the Polar-Nonpolar Segregation of the Bilayer

Ella Mihailescu[1], Jorge I. Hernandez[2], Kimberly Bogardus[3], Ashley Carducci[3], Janet Hammer[4], Jack Blazyk[4], and Myriam L. Cotten[3]

[1]Institute for Bioscience and Biotechnology Research, University of Maryland, Rockville, MD, USA
[2]Department of Bioengineering, Clemson University, Clemson, SC, USA
[3]Department of Chemistry, Hamilton College, Clinton, NY, USA
[4]Department of Biomedical Sciences, Ohio University, OH, USA

Introduction

Piscidins 1 and 3 (P1 & p3) are amphipathic, cationic, antimicrobial peptides (AMPs) with predominantly α-helical secondary structure in the presence of lipids. (1-6) They are active on a broad range of pathogens, including MRSA; P1, which is general more biologically active than P3, has anti-HIV and anti-cancer properties. (1, 7-8)

P1: FFHHIFRGIVHVGKTIHRLVTG
P3: FIHHIFRGIVHAGRSIGRFLTG

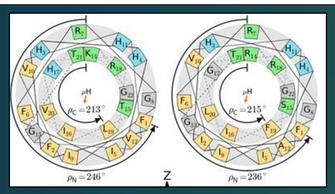

Figure 1. Helical wheel diagram comparing P1 & P3 bound to 3:1 phosphocholine/phosphoglycerate (PC/PG) aligned bilayers as determined by solid-state NMR. (1)

Research Questions:
1. What is the bilayer location of P1 and P3?
2. What are the effects of P1 and P3 on the bilayer structure?
3. Can atomic-level details help explain the stronger antimicrobial activity and permeabilization ability of P1 over P3?

Methods:
1. Dye leakage assays at Ohio University.
2. Oriented circular dichroism at Hamilton College.
3. X-ray and neutron diffraction at NIST.

Lipid system: 3:1 palmitoyloleoylphosphocholine (POPC)/1-palmitoyloleoylphosphoglycerol (POPG)

Results

Permeabilization effects: Dye leakage assays

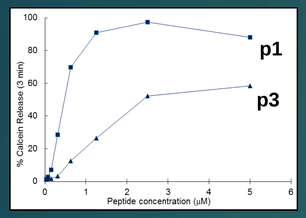

Figure 2. Membrane disruption leading to calcein release from 3:1 POPC/POPG large unilamelar vesicles when P1 (squares) and P3 (triangles) are added to the vesicles at pH 7.4.

Preliminary peptide orientation as a function of peptide content: Oriented circular dichroism

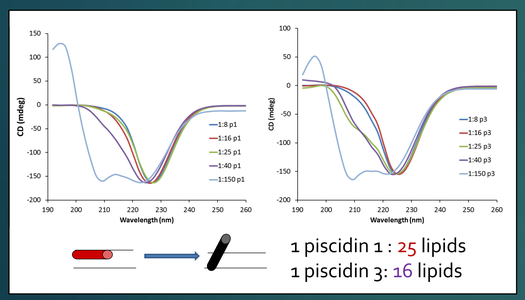

Figure 3. Oriented circular dichroism of P1 and P3 in 3:1 POPC/POPG bilayers prepared at pH 7.4 and hydrated at 93% RH. The peptide-to-lipid ratio (P/L) is increased from 1:150 to 1:8. Disappearance of the signal at 208 nm indicates insertion in the bilayer. The experiments were performed on a Jasco 815 instrument at RT.

Effects of increasing P1 content on lipid bilayer: X-ray diffraction data

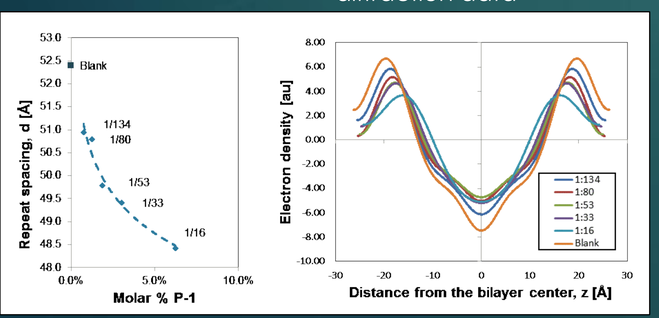

Figure 4. Determination of bilayer thickness in the presence of P1 at various P/L ratios using X-ray diffraction on POPC/POPG bilayers hydrated at 93% RH. The experiments were performed at NIST.

Out-of-plane neutron diffraction

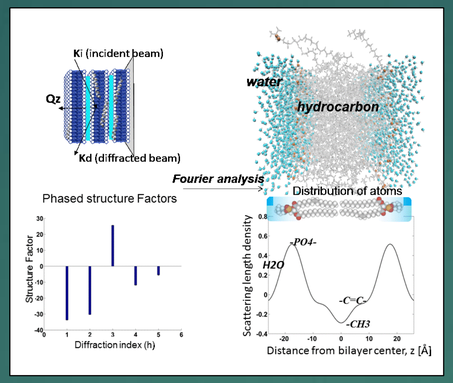

Figure 5. Out-of-plane neutron diffraction performed on bilayer systems. This technique provides detailed structural information about the bilayer structure and thickness. Phased structure factors can be analyzed to provide the location of water, phosphate headgroups, and hydrocarbon core. In this research, experiments were performed on the MAGIK instrument at NIST.

Bilayer location of P1 and P3 at a 1:25 peptide-to-lipid ratio

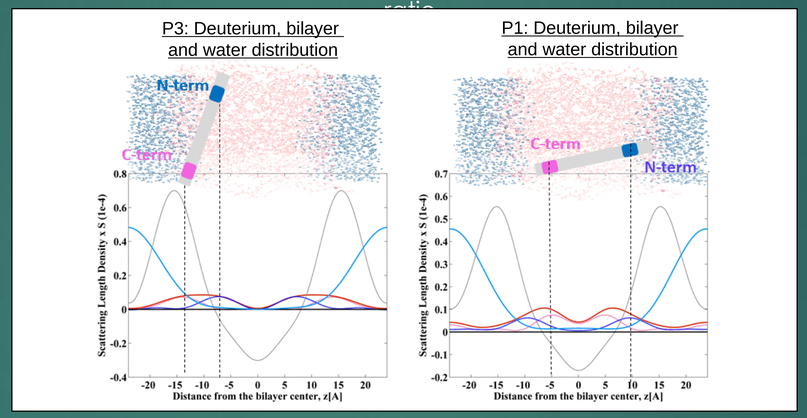

Figure 6. Scattering length density profiles for samples containing deuterated varieties of P1 (right) and P3 (left) at a 1:25 P/L. Deuterium peaks due to C-end deuterated P1 or P3 (positions 19 & 20): d-P1 or d-P3 (orange), and C-end/N-end-deuterated P1 (positions 5 & 6; 19 & 20): dd-P1 (red) are shown. Purple is the difference between the red and orange curves, pointing to the position of the N-terminus of the peptides in the bilayer. Blue and gray lines indicate the position of water and lipids, respectively.

P3: orientation and position analysis

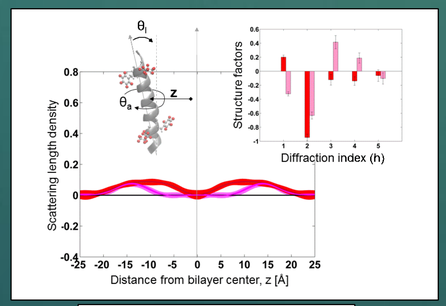

Figure 7. Orientation and position analysis of the data for P3. A Gaussian model was used for each deuterium atom, with a thermal factor (B). The rigid body transformations performed to fit the data included rotations (θ_a, θ_l) and translation (z).

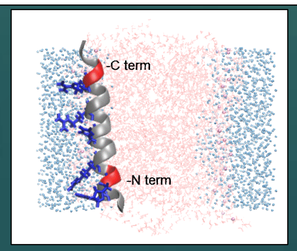

Figure 8. Unique orientation of P3 in the bilayer. P3 displays a unimodal distribution in the bilayer. The N-end is more inserted than the C-end by ~ 5.5 Å. It is found to be somewhat more tilted than the solid-state NMR structure obtained in dimyristoylphosphatidylcholine/ dimyristoylphosphoglycerol (DMPC/DMPG).

P1: Deuterium, bilayer, and water distribution

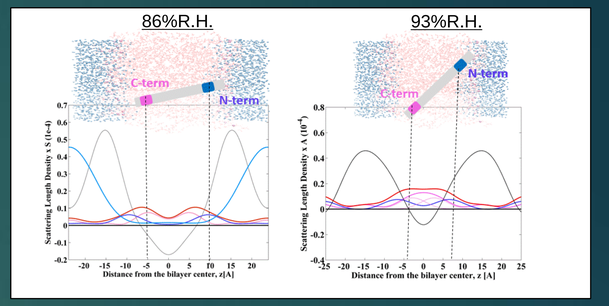

Figure 8. Scattering length density comparison for P1 at two different levels of hydration. The lower (left) and higher (right) hydration level data were obtained using P/L values of 1:25 and 1:12, respectively.

P1: Major structural perturbations caused to the lipid membranes

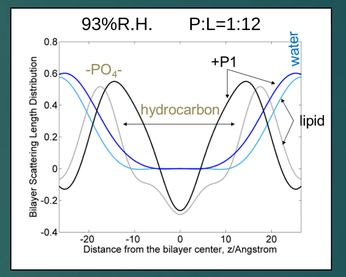

Figure 9. Analysis of the scattering length density results at higher hydration. Both the water and lipid profiles are strongly affected by the addition of P1 (full lines) in comparison to the absence of peptide (dashed lines). In particular, both the water and phosphate headgroups reach closer to the center of the bilayer. A broadening of the distribution is observed for the hydrocarbon region.

P1: Deuterium analysis suggests an inserted (across the bilayer) conformation

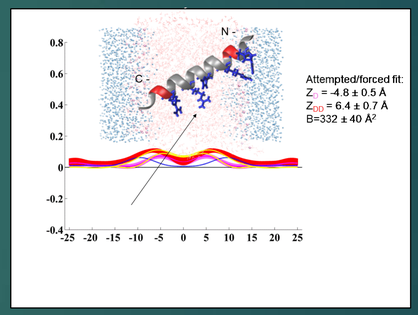

Figure 10. Location and orientation analysis of the data for P1. No unique model could be found to fit the P1 data, therefor P1 displays a multi-modal distribution. A representative conformation of P1 is shown here. These results suggest that an oligomeric state of P1 featuring various orientations of the peptide exists at high peptide content and hydration.

Conclusions

- X-ray and neutron diffractions are a powerful technique to investigate membrane-bound peptides under varying conditions
- P3, the less membrane-active piscidin isoform, is surface bound.
- P1, the more active form, is inserted and induces major structural rearrangements of the membrane. An oligomeric state is very likely.

Acknowledgments

The authors acknowledge the National Institute of Standards and Technology for instrument time. We thank the National Science Foundation (CHE 0832571) for their financial support and continued dedication to research and education.

References

(1) Perrin, B.S., …, Cotten , M. J. *Am. Chem. Soc.* **2014,**136:3491-3504.
(2) Chekmenev, E.Y., …, Cotten, M. *Biochim Biophys Acta* **2006**, 1758:1359-1372.
(3) Chekmenev, E.Y., …, Cotten, M. J. *Am. Chem. Soc.* **2009,**131:10830-10831.
(4) Chekmenev, E.Y., … Cotten, M. *Biochim. Biophys. Acta.* **2010**, 1798:228-234.
(5) Fu, R.; Gordon, E.D.; Hibbard, D.J.; and Cotten, M. J. *Am. Chem. Soc.* **2009**, 131:10830–10831.
(6) De Angelis A.A.; Grant C.V.; Baxter, M.K.; McGavin, J.A.; Opella, S.J.; Cotten, M.L. **Biophys. J. 2011**, 101:1086-1094.
(7) (a) Noga, E. J.; Silphaduang, U. *Drug News Perspect.* **2003**, 16:87-92. (b) Lauth *et al. J. Biol. Chem.* 2002, 277:5030-5039.
(8) Campagna, S.; Saint, N.; Molle, G.; Aumelas, A. *Biochemistry* **2007,** 46:1771-1778.
(9) Han, X.; Mihailescu, M.; Hristova, K. *Biophys J.* **2006**, 9:3736-3637.